Neuro-Oncology
23(7), 1183–1196, 2021 | doi:10.1093/neuonc/noab016 | Advance Access date 4 February 2021

OLIG2 maintenance is not essential for diffuse intrinsic pontine glioma cell line growth but regulates tumor phenotypes

Yunfei Liao,[†] Zaili Luo,[†] Yaqi Deng, Feng Zhang, Rohit Rao, Jiajia Wang, Lingli Xu, Shiva Senthil Kumar, Satarupa Sengupta, Mariko DeWire-Schottmiller, Kalen Berry, Matthew Garrett, Maryam Fouladi,[1] Rachid Drissi,[2] and Qing Richard Lu

Brain Tumor Center, Division of Experimental Hematology and Cancer Biology, Cincinnati Children's Hospital Medical Center, Cincinnati, Ohio, USA (Y.L., Z.L., Y.D., F.Z., R.R., J.W., L.X., S.S.K., S.S., M.D.S., K.B., M.F., R.D., Q.R.L.); Department of Pediatrics, University of Cincinnati College of Medicine, Cincinnati, Ohio, USA (Q.R.L.); Department of Neurosurgery, University of Cincinnati College of Medicine, Cincinnati, Ohio, USA (M.G.)

Corresponding Author: Rachid Drissi, PhD, Brain Tumor Center, Division of Experimental Hematology and Cancer Biology, Cincinnati Children's Hospital Medical Center, Cincinnati, OH 45229, USA (rachid.drissi@nationwidechildrens.org); Dr. Qing Richard Lu, PhD, Brain Tumor Center, Division of Experimental Hematology and Cancer Biology, Cincinnati Children's Hospital Medical Center, Cincinnati, OH 45229, USA (richard.lu@cchmc.org).

[1]**Present affiliation:** Pediatric Neuro-Oncology Program, the Ohio State University College of Medicine, Nationwide Children's Hospital, Columbus, OH, USA.
[2]**Present affiliation:** Center for Childhood Cancer & Blood Disorders, the Ohio State University College of Medicine, Nationwide Children's Hospital, Columbus, OH, USA.

[†]These authors contributed equally to this work.

Abstract

Background. Diffuse intrinsic pontine glioma (DIPG) is a pediatric lethal high-grade brainstem glioma with no effective therapies. OLIG2 (oligodendrocyte transcription factor 2) was reported to be critical for the growth of a DIPG cell line CCHMC-DIPG-1. Surprisingly, we found that the CCHMC-DIPG-1 cells express little OLIG2 and exhibit a mesenchymal phenotype, which raised a question regarding the role of OLIG2 in the growth of DIPG cells.

Methods. We evaluated the function of OLIG2 in different DIPG cell lines through molecular and genetic approaches and performed transcriptomic and genomic landscape profiling including whole-genome bisulfite sequencing, RNA-seq, ATAC-seq, and ChIP-seq. shRNA-mediated knockdown and CRISPR-Cas9-mediated knockout approaches were utilized to assess OLIG2 functions in DIPG cell growth.

Results. We found that DIPG cells are phenotypically heterogeneous and exhibit the characteristics of distinct malignant gliomas including proneural, classical, and mesenchymal subtypes. OLIG2 knockdown did not impact the growth of CCHMC-DIPG-1 cells, wherein *OLIG2* is epigenetically silenced. Moreover, *OLIG2* deletion did not substantially impair OLIG2-expressing proneural-like DIPG growth but led to an upregulation of HIPPO-YAP1 and epidermal growth factor receptor (EGFR) signaling and a tumor phenotype shift. Targeting HIPPO-YAP1 and EGFR signaling in OLIG2-deficient DIPG cells inhibited tumor cell growth.

Conclusions. Our data indicate that OLIG2 is dispensable for DIPG growth but regulates the phenotypic switch of DIPG tumor cells. OLIG2 downregulation leads to deregulation of adaptive YAP1 and EGFR signaling. Targeting YAP1 and EGFR pathways inhibits the growth of OLIG2-deficient DIPG cells, pointing to a therapeutic potential by targeting adaptive signaling to treat DIPG tumors with nominal OLIG2 expression.

Key Points

1. DIPGs exhibit distinct tumor phenotypes but OLIG2 is not essential for their growth.
2. OLIG2 downregulation leads to a tumor phenotype shift of DIPG cells.
3. Targeting YAP1 and EGFR signaling inhibits OLIG2-deficient DIPG cell growth.

Importance of the Study

Our findings indicate that DIPG cells exhibit distinct tumor phenotypes. Although OLIG2 expression can be detected in proneural DIPG cells, a set of DIPG cells express little to no OLIG2 and exhibit a mesenchymal-like or classical-like tumor phenotypes. In contrast to the previous report, we found that the growth of CCHMC-DIPG-1 cells is independent of OLIG2 expression. In addition, deletion of *OLIG2* in OLIG2-expressing proneural-like DIPG cells does not substantially inhibit tumor cell growth. Rather lack of OLIG2 causes a shift of proneural-like phenotype toward an OLIG2-low mesenchymal-like or a classical phenotype with YAP1 and EGFR signaling upregulation, which confers therapeutic vulnerabilities. Combined targeting of adaptive YAP1 and EGFR signaling effectively inhibited the growth of DIPG cells with negligible-OLIG2. Understanding the vulnerability of distinct DIPGs is important for patient stratification and for the development of new therapies to treat aggressive DIPGs.

Diffuse intrinsic pontine glioma (DIPG), also known as diffuse midline glioma, arises from the midline of the brain located close to the centers controlling vital functions and primary sensorimotor axons rendering them inoperable. DIPGs are fatal tumors, which are inoperable and resistant to chemo- and radiotherapy, representing a leading cause of brain tumor-associated death in children with a median survival of only 8-11 months.[1,2] DIPG tumors are highly heterogeneous with distinct molecular signatures. Genomic analysis revealed that a majority of DIPG tumors harbor a lysine 27 to methionine (K27M) mutation in histone H3.3 or H3.1 (H3.3 K27M and H3.1 K27M, respectively),[1,3–6] although a subset of DIPG tumors have wild-type histone H3.3. In addition, amplification of *PDGFRA*, which is correlated with oligodendrocyte precursor cell (OPC) proliferation, occurs in the majority of DIPG patients.[7–9] Neonatal induction of H3.3 K27M promotes self-renewal in the neural progenitors and, in cooperation with *PDGFRA* amplification and *p53* loss, accelerates the malignant transformation of neural progenitors into DIPG-like tumors in a murine model of DIPG.[10,11]

Based on gene expression patterns, malignant high-grade gliomas such as glioblastomas (GBM) can be classified into distinct subtypes exhibiting proneural, classical, and mesenchymal phenotypes.[12] The proneural subtype is associated with an oligodendrocyte lineage signature, eg, with expression of an oligodendrocyte lineage gene *OLIG2*, the classical subgroup is strongly associated with the astrocytic lineage, eg, with expression of epidermal growth factor receptor (EGFR), and the mesenchymal subgroup is associated with pathways including YAP1, TGF-β, and NF-κB signaling.[12] Stem-like progenitors and/or OLIG2$^+$ OPC-like progenitors in the pons have been suggested as a cell of origin for DIPG tumors.[4,5,13] Recent genome-wide transcriptional and single-cell transcriptomic analyses of DIPGs revealed a prominent OPC-like population with a stemness-associated signature.[14–18]

OLIG2 (oligodendrocyte transcription factor 2) has been shown to regulate *PDGFRA* expression during oligodendrocyte lineage development.[19,20] OLIG2 is also expressed in early primitive OPCs (eg, pri-OPC or pre-OPC) exhibiting the stemness signature in malignant gliomas and DIPGs.[17,21,22] OLIG2 expression can be detected in DIPG tumors, however, some DIPGs express very low levels or no OLIG2.[8,18,23] Although the subclassification of OLIG2 expression in DIPG gliomas is not fully defined, given the similar nature of high-grade gliomas between DIPGs and GBM tumors, OLIG2 expression is likely enriched in the proneural subgroup tumors but exhibits low levels or is absent entirely in classical or mesenchymal tumors.[12] The existence of classical and mesenchymal-like DIPGs and GBM tumors with marginal *OLIG2* expression suggests a nonessential function of OLIG2 in the growth of these subtypes of malignant gliomas complemented by other as yet unidentified pathways.

A recent study by Anderson et al. reported that shRNA-mediated *OLIG2* knockdown in a DIPG cell line CCHMC-DIPG-1 (referred to here as CC-DIPG-1) inhibits tumor cell growth in vitro and tumor formation in xenografts, concluding an important requirement for OLIG2 in the growth of these cells.[24] However, unexpectedly, we found that the CC-DIPG-1 cell line exhibits minimal *OLIG2* expression and manifests a mesenchymal tumor phenotype. Whole-genome DNA methylation analysis revealed that the promotor region of *OLIG2* was heavily methylated in CC-DIPG-1 cells, while DNA demethylation treatment led to upregulation of OLIG2, suggesting that *OLIG2* expression is intrinsically silenced by hypermethylation in CC-DIPG-1 cells. We further showed that targeting residual *OLIG2* using an shRNA did not inhibit the growth of CC-DIPG-1 cells; this is in contrast to the reported essential role of OLIG2 in CC-DIPG-1 growth.[24] Transcriptomics profiling reveals distinct tumor phenotypes in DIPGs, similar to GBM. Strikingly, we uncovered a strong upregulation of

EGFR and YAP1 signaling in the OLIG2-nominal CC-DIPG-1 line and OLIG2-knockout (KO) DIPG cell lines. Elevation of EGFR and YAP1 in the OLIG2-deficient cells likely sustains cell growth and proliferation of OLIG2-deficient DIPG cells. Inhibition of YAP1 and EGFR signaling impaired the growth of OLIG2-deficient DIPG cells, suggesting that targeting YAP1 and EGFR signaling may sensitize DIPG tumor cells that have low or negligible levels of OLIG2 to the pathway inhibition. Thus, our studies suggest a potential strategy for the treatment of OLIG2-low DIPG tumors.

Methods

Patient-Derived DIPG Cell Lines

All human cell cultures were generated with informed consent and in compliance with Institutional Review Board (IRB)-approved protocols at Cincinnati Children's Hospital Medical Center. CCHMC-DIPG-1 (H3.3-wild type, not H3.3-K27M as stated in the previous report[24]) and CCHMC-DIPG2 (H3.3-K27M) cells were cultured at the time of autopsy in two different subjects, respectively. Patient-derived primary SU-DIPG series cell lines are the gift from Dr. Michelle Monje at Stanford University[18] as described in the Supplementary Methods.

Cell Culture, Proliferation, and Invasion Assays

The DIPG cell lines were cultured as previously reported.[25] Cell proliferation was assayed using WST-1 cell proliferation assay kit (Roche, 5015944001). Cell invasion was assessed by Boyden Chamber assay (BD Biosciences). See the Supplementary Methods for details.

Subcutaneous Transplantation

NOD scid gamma (NSG) mice were from CCHMC animal core. DIPG cells were subcutaneously transplanted into the flank of NSG mice. All procedures were performed according to the Institutional Animal Care and Use Committee approved protocol at CCHMC. See the Supplementary Methods for details.

Gene Knockdown and KO in DIPG Cell Lines

Gene knockdown and KO in DIPG cell lines were generated by using lenti-pGreenPuro shRNA (SBI System Biosciences) and Lenti-CRISPRv2 (Addgenes 52961) vectors, respectively. See the Supplementary Methods for details.

Immunochemistry

Cryosections from tumor tissues or neurospheres, or cultured cells on the coverslips were immunostained with primary antibodies (anti-OLIG2, YAP1, EGFR, SOX2, or BrdU), followed by fluorescence-conjugated secondary antibodies and 4′,6-diamidino-2-phenylindole (DAPI) counterstaining as described previously.[21] See the Supplementary Methods for details.

Western Blotting and Quantitative RT-PCR

For western blotting, DIPG cells were lysed in radioimmunoprecipitation assay buffer with protease and phosphatase inhibitors. Proteins were separated via 12% SDS-polyacrylamide gel electrophoresis. Antibodies are listed in the Supplementary Materials. For quantitative RT-PCR (qRT-PCR), RNAs were extracted from DIPG cells using TRIzol Reagent (Life Technologies). cDNA was synthesized from RNA using iScript Reverse Transcription Supermix (Bio-Rad, #1708 841). qRT-PCR was performed using the StepOnePlus Real-Time PCR System (Applied Biosystems). See the Supplementary Methods for details.

RNA-Seq, ATAC-Seq, ChIP-Seq, DNA Methylation, and Data Analysis

RNAs of DIPG cells were extracted using the RNeasy Mini Kit (Qiagen) and RNA-seq libraries were prepared using Illumina RNA-Seq Preparation Kit and sequenced by a HiSeq 2500 sequencer. RNA-Seq data were analyzed by alignment to hg19 using TopHat with default settings as described previously.[21] ChIP-Seq and ATAC-Seq were performed as previously described.[21,26] For ATAC-seq and ChIP-seq, the sequencing data were aligned to hg19 genome assembly and the peak calling was generated by using model-based analysis of ChIP-seq (MACS; https://github.com/macs3-project/MACS). Whole-genome DNA methylation profiling was analyzed using reduced representation bisulfite sequencing (RRBS).[27] Integrative Genomics Viewer (IGV) (https://igv.org) was used to read the peaks of target genes. See the Supplementary Methods for details.

Statistical Methods

Detailed information of all the statistical analyses performed is described in the Supplementary Methods.

Results

OLIG2 Expression Is Barely Detectable in CC-DIPG-1 Cells In Vitro and In Vivo

While investigating the expression level of *OLIG2* in DIPG cell lines by qRT-PCR analysis, we found that expression of *OLIG2* in CC-DIPG-1 was minimal, in contrast to robust *OLIG2* expression in CCHMC-DIPG2 (CC-DIPG-2), SU-DIPG-IV, SU-DIPG-VI, and SU-DIPG-XIII lines[28] (Figure 1A). This is in contrast to a previous report of robust OLIG2 expression in CC-DIPG-1 cells.[24] To validate the observation at the protein level, we performed western blot analysis and showed that OLIG2 protein expression was negligible in a set of DIPG cells including CC-DIPG-1 and SU-DIPG-XXXVI cells, as well as human astrocytes, whereas staining was intense in SU-DIPG-IV, SU-DIPG-XIII, and CC-DIPG-2 cells (Figure 1B). Moreover, immunofluorescence

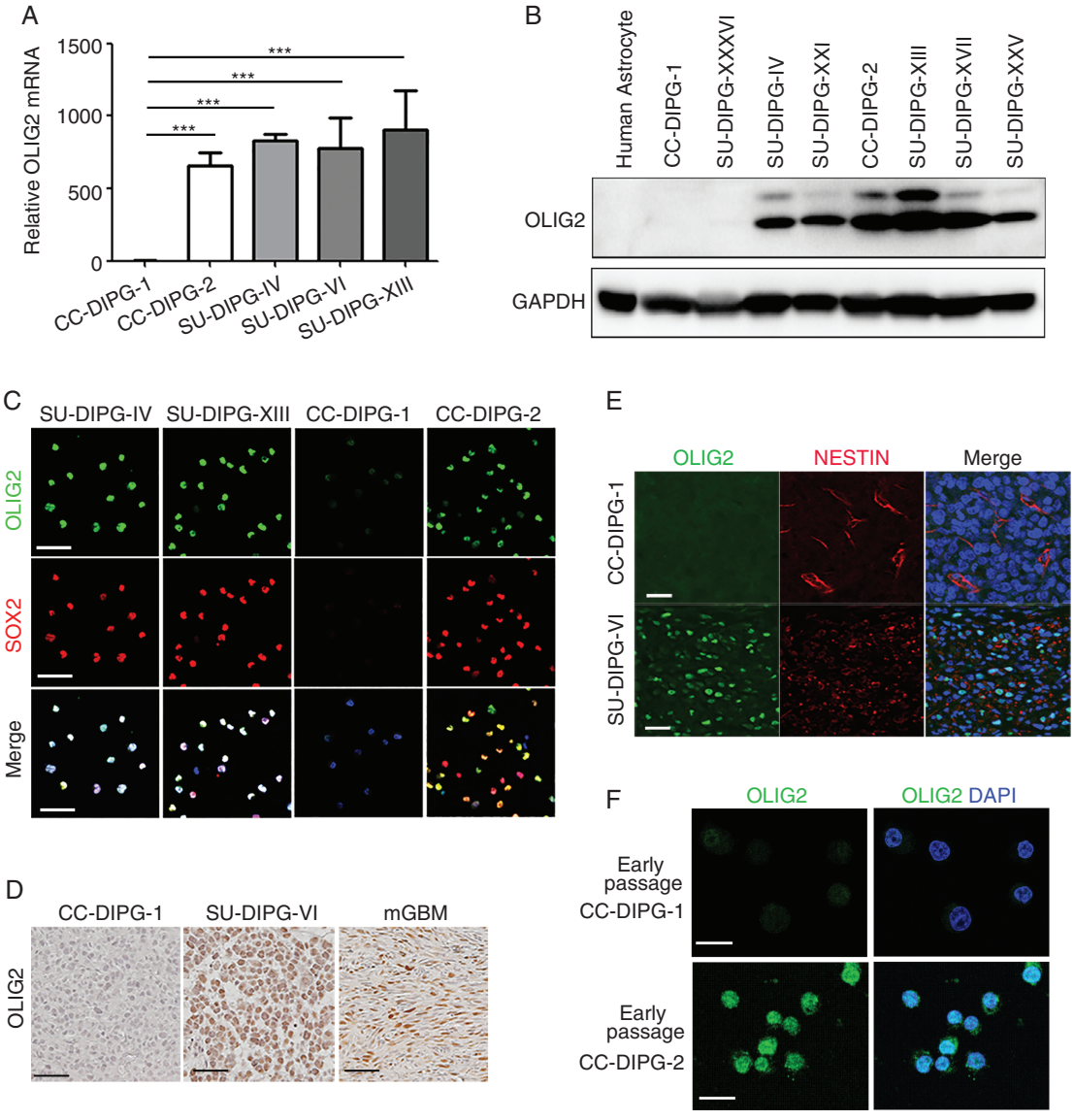

Fig. 1 OLIG2 expression low in CC-DIPG-1 cells in vitro and in vivo. (A) qRT-PCR analysis of *OLIG2* in CC-DIPG-1, DIPG-2, DIPG-IV, DIPG-VI, and DIPG-XIII cells cultured in serum-free DIPG stem cell medium. Data are presented as means ± SEM; n = 3 experiments; ***$P < .001$; one-way ANOVA with multiple comparisons test. (B) Western blot of OLIG2 expression in CC-DIPG-1, DIPG-2, DIPG-IV, and DIPG-XIII cells. (C) Confocal immunofluorescence microscopy images SU-DIPG-XIII, SU-DIPG-IV, CC-DIPG-1, and CC-DIPG-2 cells stained for OLIG2 (green) and SOX2 (red). (D) Immunohistochemistry analyses of xenografts of CC-DIPG-1, SU-DIPG-VI, and mGBM for expression of OLIG2. (E) Confocal immunofluorescence images of xenografts of CC-DIPG-1 and SU-DIPG-VI stained for OLIG2 (green) and NESTIN (red). (F) Confocal immunofluorescence microscopy images of CC-DIPG-1 cells and CC-DIPG-2 cells at low passage stained for OLIG2 (green). Scale bars in C-E, 50 µm; F, 25 µm. Abbreviations: DIPG, diffuse intrinsic pontine glioma; mGBM, multifocal glioblastoma; OLIG2, oligodendrocyte transcription factor 2; qRT-PCR, quantitative RT-PCR.

staining indicated that OLIG2 and stemness marker SOX2 were barely detected in CC-DIPG-1 cells compared with robust expression in SU-DIPG-IV, SU-DIPG-XIII, and CC-DIPG-C2 cell lines (Figure 1C).

To investigate OLIG2 expression in DIPG xenografts in vivo, we transplanted CC-DIPG-1 cells, SU-DIPG-VI cells, and mGBM cells (a mouse glioma cell line) into the flanks of NSG mice. OLIG2 expression was detected in the SU-DIPG-VI and mGBM tumors (Figure 1D), but, in contrast to the previous report,[24] OLIG2 was hardly detected by immunofluorescence or by immunohistochemistry staining in CC-DIPG-1 xenografts (Figure 1D and E).

To determine if the passaging of CC-DIPG-1 cells had led to the loss of OLIG2 expression, we examined OLIG2 expression in the early passage CC-DIPG-1 cells obtained from the tumor isolated from the DIPG patient. OLIG2 was barely detected in these cells by immunostaining (Figure 1F). These data suggest minimal OLIG2 expression is intrinsic to CC-DIPG-1 cells.

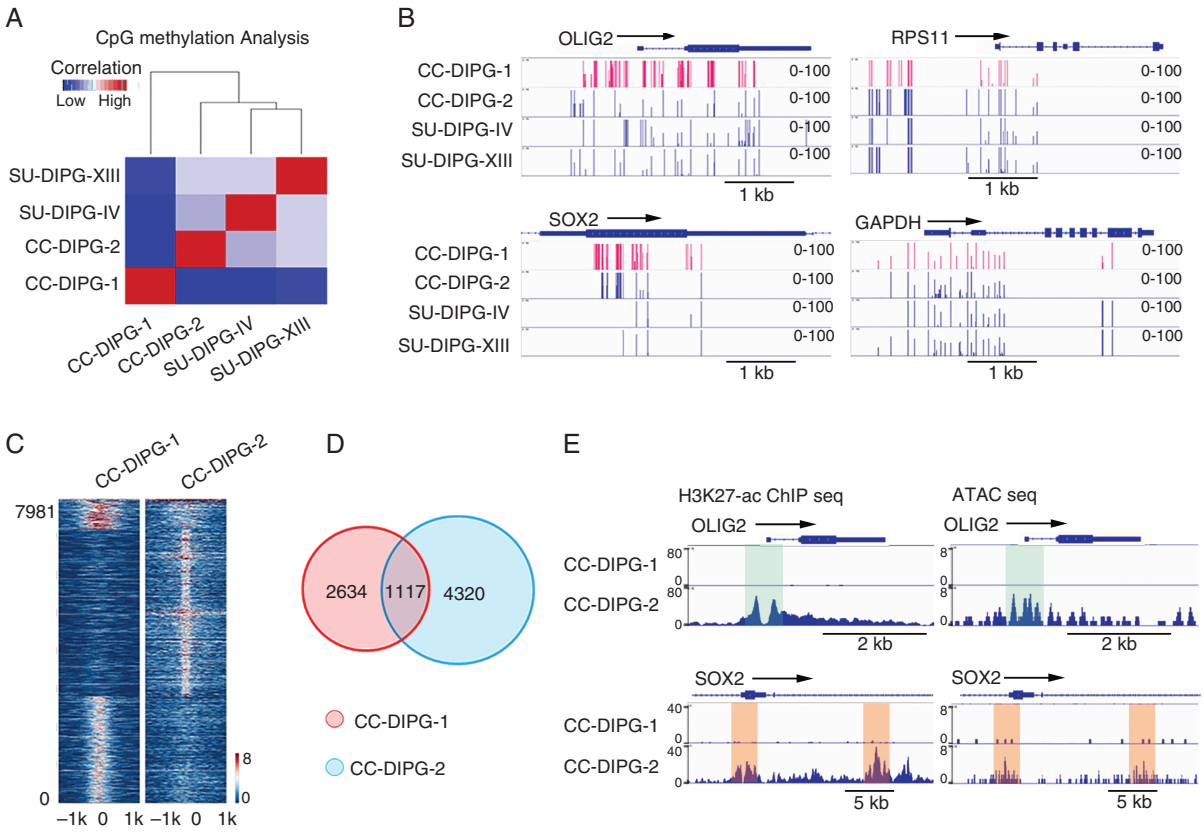

Fig. 2 OLIG2 is epigenetically silenced in CC-DIPG-1 cells. (A) CpG methylation clustering analysis of SU-DIPG-IV, SU-DIPG-XIII, CC-DIPG-1, and CC-DIPG-2 cells. (B) Diagram showing CpG methylation signals at *OLIG2*, *SOX2*, and control gene (*RPS11* and *GAPDH*) loci in DIPG cell lines. (C) Heatmap of signal intensities of ATAC-seq peaks in CC-DIPG-1 and CC-DIPG-2. (D) Venn diagraph of signal intensities of ATAC-seq peaks from CC-DIPG-1 and CC-DIPG-2 cells. (E) Chromatin accessibility and H3K27ac ChIP-seq profiles at *OLIG2* and *SOX2* loci in CC-DIPG-1 and CC-DIPG-2 cells. Abbreviations: DIPG, diffuse intrinsic pontine glioma; OLIG2, oligodendrocyte transcription factor 2.

Genome-Wide DNA Methylation Analysis Reveals That *OLIG2* Is Epigenetically Silenced in CC-DIPG-1 Cells

DNA methylation can result in a repressed chromatin state that inhibits gene transcription.[29] To investigate the genomic DNA methylation landscape of the CC-DIPG-1 cells, we performed whole-genome bisulfite sequencing of DIPG cell lines. The genome-wide methylation pattern of CC-DIPG-1 was distinguished from that of SU-DIPG-IV, SU-DIPG-XIII, and CC-DIPG-2 cells (Figure 2A). The pairwise Pearson's correlation analysis indicated that the DNA methylation patterns of SU-DIPG-IV and CC-DIPG-2 cells were closely related but distinct from that of CC-DIPG-1 cells (Figure 2A). We found that in promoters and gene bodies of *OLIG2* and *SOX2*, CpG sites were hypermethylated in CC-DIPG-1 cells compared with SU-DIPG-IV, SU-DIPG-XIII, and CC-DIPG-2 cells (Figure 2B). The hypermethylation on the promotor region of *OLIG2* indicates a transcriptionally silenced state for OLIG2 transcription.

To test whether DNA demethylation would increase OLIG2 expression in CCHMC-DIPG-1 cells, we treated CCHMC-DIPG-1 cells with a DNA demethylating agent decitabine. qRT-PCR and western blot analyses showed that the expression level of OLIG2 mRNA and protein increased in response to the treatment in a dose-dependent manner (Supplementary Figure S1A and B). This observation is consistent with a previous report that decitabine treatment resulted in re-expression of OLIG2 in non-OLIG2-expressing acute myeloid leukemia cells.[30] Our results suggest that DNA hypermethylation in the promoter/enhancer elements of OLIG2 at least in part leads to epigenetic silencing of OLIG2 expression in the CCHMC-DIPG-1 cells.

To further assess the chromatin accessibility landscape in DIPG cells, we performed the ATAC-seq assay, which identifies transposase-accessible chromatin.[26] ATAC-seq results revealed distinct patterns of chromatin accessibility between CC-DIPG-1 and CC-DIPG-2 cells (Figure 2C and D). The open chromatin regions such as the *OLIG2* and *SOX2* loci in the CC-DIPG-2 cells were closed in CC-DIPG-1 cells (Figure 2E). Consistent with these findings, ChIP-sequencing analysis of an activating histone mark H3K27ac showed that this mark was present on the promoter regions of *OLIG2* and *SOX2* in CC-DIPG-2 cells but not in CC-DIPG-1 cells (Figure 2E). These observations indicate that the chromatin regions in the gene loci of *OLIG2*

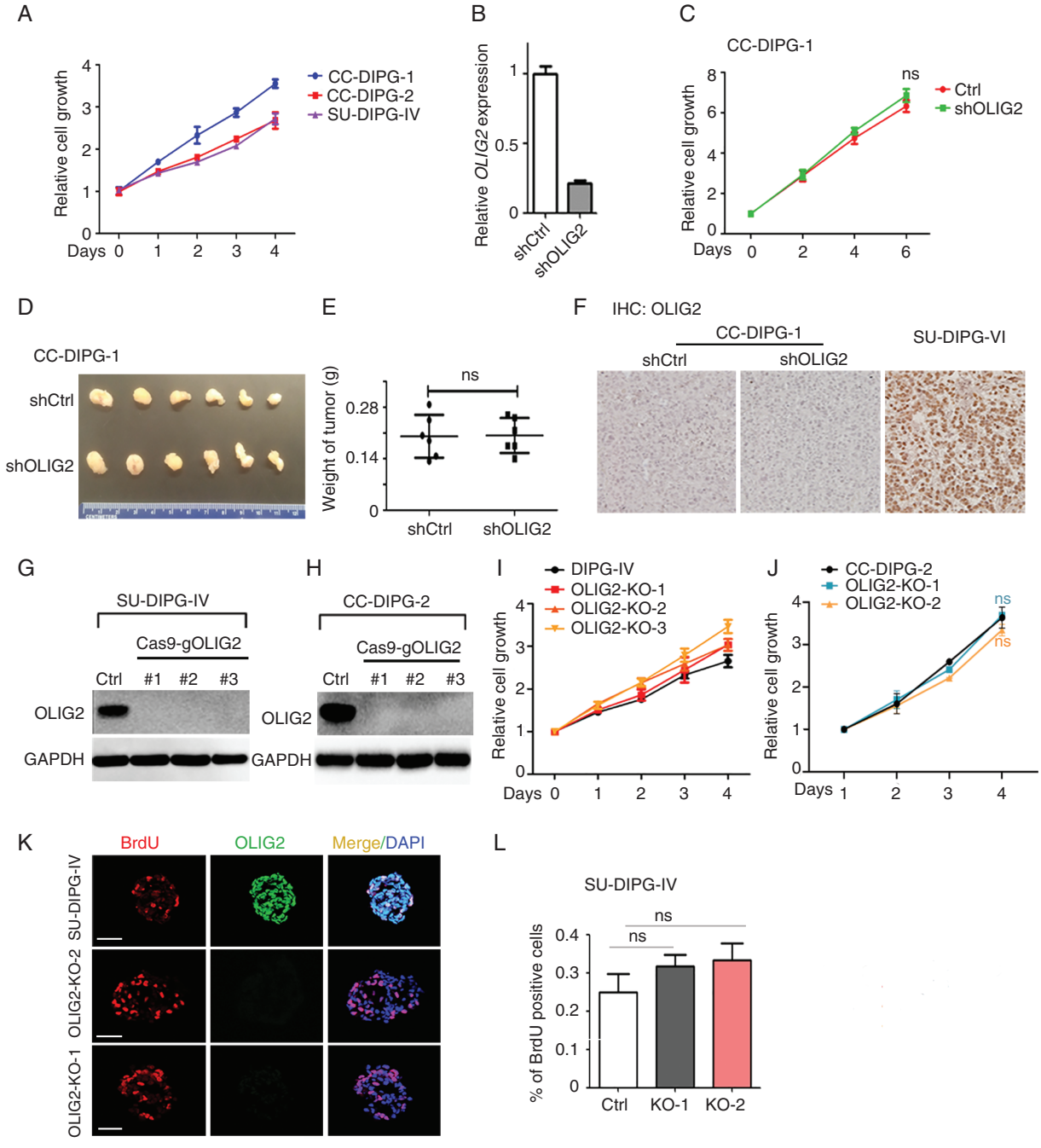

Fig. 3 OLIG2 is not required for tumorigenesis and proliferation of DIPG cells. (A) The growth of DIPG cell lines tested by WST-1 assay. (B) qRT-PCR validation of shOLIG2-mediated *OLIG2* depletion. (C) Cell growth of CC-DIPG-1 cells treated with lenti-shCtrl or shOLIG2 tested by WST-1 assay. (D) Photomicrographs of tumors formed in flanks of NSG mice implanted with CC-DIPG-1 cells transfected with lenti-shCtrl or lenti-shOLIG2. N = 6 animals/group. (E) Weights of tumors formed in flanks of NSG mice injected with CC-DIPG cells that had been transfected with lenti-shCtrl or lenti-shOLIG2. (F) Tumors stained for OLIG2 from mice injected with CC-DIPG-1 cells that had been transfected with control or lenti-shOLIG2 and from mice injected with DIPG-VI cells. (G, H) Representative western blots for OLIG2 in wild-type and *OLIG2*-KO SU-DIPG-IV (G) and CC-DIPG-2 (H) cells. (I, J) Cell growth of wild-type and *OLIG2*-KO SU-DIPG-IV (I) and CC-DIPG-2 (J) cells determined by WST-1 assay. (K, L) BrdU (K) staining and quantification (L) of wild-type and *OLIG2*-KO SU-DIPG-IV cell neurospheres after 2 h of BrdU labeling. Scale bars in F, 100 μm; K, 50 μm. Abbreviations: DIPG, diffuse intrinsic pontine glioma; mGBM, multifocal glioblastoma; NSG, NOD scid gamma; OLIG2, oligodendrocyte transcription factor 2; qRT-PCR, quantitative RT-PCR.

and *SOX2* are hardly accessible in CC-DIPG-1 cells and that these genes are silenced in CC-DIPG-1 cells. Together, these observations of the hyper-DNA methylation and closed chromatin state at the promoter region of *OLIG2* locus suggest that OLIG2 expression in CC-DIPG-1 is inherently repressed.

OLIG2 Depletion Does Not Affect the Growth of CC-DIPG-1 Cells In Vitro or In Vivo

To assess proliferation of CC-DIPG-1 cells, we performed the WST-1 assay for cell proliferation and survival. Intriguingly, we found that OLIG2-deficient CC-DIPG-1 cells appeared to grow more rapidly than OLIG2-positive DIPG cell lines such as SU-DIPG-IV and CC-DIPG-2 (Figure 3A). The previous study reported that knockdown of *OLIG2* in the CC-DIPG-1 cells reduced tumor growth.[24] To further determine whether the residual OLIG2 expression in CC-DIPG-1 cells was required for proliferation, we transduced CC-DIPG-1 cells with a lentivirus expressing an shRNA designed to target *OLIG2* (lenti-shOLIG2) or with a control non-targeted shRNA vector. The expression of the shRNA targeting *OLIG2* further reduced the residual level of *OLIG2* mRNA in CC-DIPG-1 cells (Figure 3B). In the WST-1 cell proliferation assay, there was not a significant difference between the growth of CC-DIPG-1 cells treated with control and lenti-shOLIG2 (Figure 3C). Similarly, *OLIG2* knockdown did not affect the growth of another OLIG2-deficient SU-DIPG-XXXVI cells (Supplementary Figure S2A).

To investigate whether there is a difference in tumor growth in vivo after OLIG2 depletion of CC-DIPG-1 cells, we subcutaneously transplanted the CC-DIPG-1 cells (4×10^5) treated with lenti-control and shOLIG2 into NSG mice. Both resulted in tumors in NSG mice with 100% penetrance (Figure 3D). The tumor weights were comparable in xenografts between the CC-DIPG-1 cells that expressed lenti-control and shOLIG2 (Figure 3E). OLIG2 expression was barely detectable in CC-DIPG-1 cells transduced with either lenti-control or shOLIG2 by immunocytochemistry (Figure 3F). These data confirmed that OLIG2 is not required for the growth of CC-DIPG-1 cells in vitro or as xenografts, contrasting with the previous report that OLIG2 was necessary for the growth of these cells.[24]

OLIG2 Deletion Does Not Affect the Proliferation of DIPG Cells

Our observation that growth is not impaired in OLIG2-deficient CC-DIPG-1 cells prompted us to determine whether OLIG2 is required for the growth of other OLIG2$^+$ DIPG cell lines. We used a lenti-CRISPR-Cas9-sgRNA system[31] to KO *OLIG2* in OLIG2-expressing DIPG lines, SU-DIPG-IV and CC-DIPG-2. Cells were transduced with a retrovirus carrying a doxycycline-inducible lenti-Cas9-sgRNA against *OLIG2* that also expresses a Green fluorescent protein (GFP) reporter. After doxycycline treatment, GFP$^+$ single cells were sorted into 96-well plates to select individual *OLIG2*-KO clones. Selected *OLIG2*-KO clones were validated for *OLIG2* gene deletion by both Sanger DNA sequencing and western blot analyses (Figure 3G and H; Supplementary Figure S3).

To compare the growth between cells that express *OLIG2* and *OLIG2*-KO cell lines, we assessed cell proliferation using the WST-1 cell proliferation assay. KO of *OLIG2* in SU-DIPG-IV and CC-DIPG-2 cells did not decrease proliferation rates (Figure 3I and J). This is in contrast to the previous report that *OLIG2* knockdown substantially reduced the proliferation of SU-DIPG-IV cells.[24] Similar to the observations in vitro, deletion of *OLIG2* in SU-DIPG-IV or CC-DIPG-2 cell lines did not significantly alter tumor cell proliferation compared to the parental cells as assayed by BrdU incorporation (Figure 3K and L). These data support the conclusion that OLIG2 maintenance is not essential for proliferation in the set of OLIG2-expressing DIPG cells tested.

To investigate the effect of OLIG2 KO on cell-invasive behaviors, we utilized a Boyden chamber assay to examine cell invasion of OLIG2-WT and OLIG2-KO SU-DIPG4 cells and found that that there was no significant difference between OLIG2-WT and OLIG2-KO cells in terms of cell invasiveness (Supplementary Figure S4A and B). However, OLIG2-deleted DIPG cells exhibit an increase in cell adhesiveness and a decrease in tumorsphere formation compared with OLIG2-WT cells (Supplementary Figure S4C), which is in keeping with the phenotypic shift of *OLIG2*-depleted glioma cells as previously reported.[21] These observations suggest that OLIG2 is not required for DIPG cell invasiveness but regulates cell adhesiveness.

CC-DIPG-1 Exhibits a Mesenchymal-Like Phenotype With Upregulation of YAP1 and EGFR

Given that CC-DIPG-1 cells exhibit DNA methylation and chromatin accessibility patterns that differ from those of other DIPG cell lines, we hypothesized that the transcriptome of CC-DIPG-1 cells would also be distinct. We performed RNA-seq transcriptome profiling of DIPG cell lines and compared the data to transcriptomes of human neural stem cells (Figure 4A). The transcriptomic profile of CC-DIPG-1 is unique when compared to that of OLIG2-positive DIPG cells CC-DIPG-2, SU-DIPG-IV, and SU-DIPG-XIII (Figure 4A). When compared with signature genes of GBM subtypes[12] (Supplementary Table 1), OLIG2-positive DIPG cell lines have gene expression patterns similar to that of the proneural subgroup, whereas the CC-DIPG-1 expression pattern closely resembles the mesenchymal subgroup in GBM (Figure 4B and C). SU-DIPG-XIV and SU-DIPG-XXXIII tumors, which also have low or negligible levels of OLIG2 expression, resemble the classical and mesenchymal subgroup of GBM, respectively (Supplementary Figure S5). Pathway analysis indicated that classical and mesenchymal tumor-associated pathways such as EGFR, YAP, and NF-κB signaling were elevated in OLIG2-nominal CC-DIPG-1 cells compared with OLIG2-expressing DIPG cells (Figure 4D). Consistent with these findings, gene set enrichment analysis (GSEA) of gene expression revealed stronger EGFR and YAP1 signaling in CC-DIPG-1 cells compared with the other OLIG2-positive cells evaluated (Figure 4E and F).

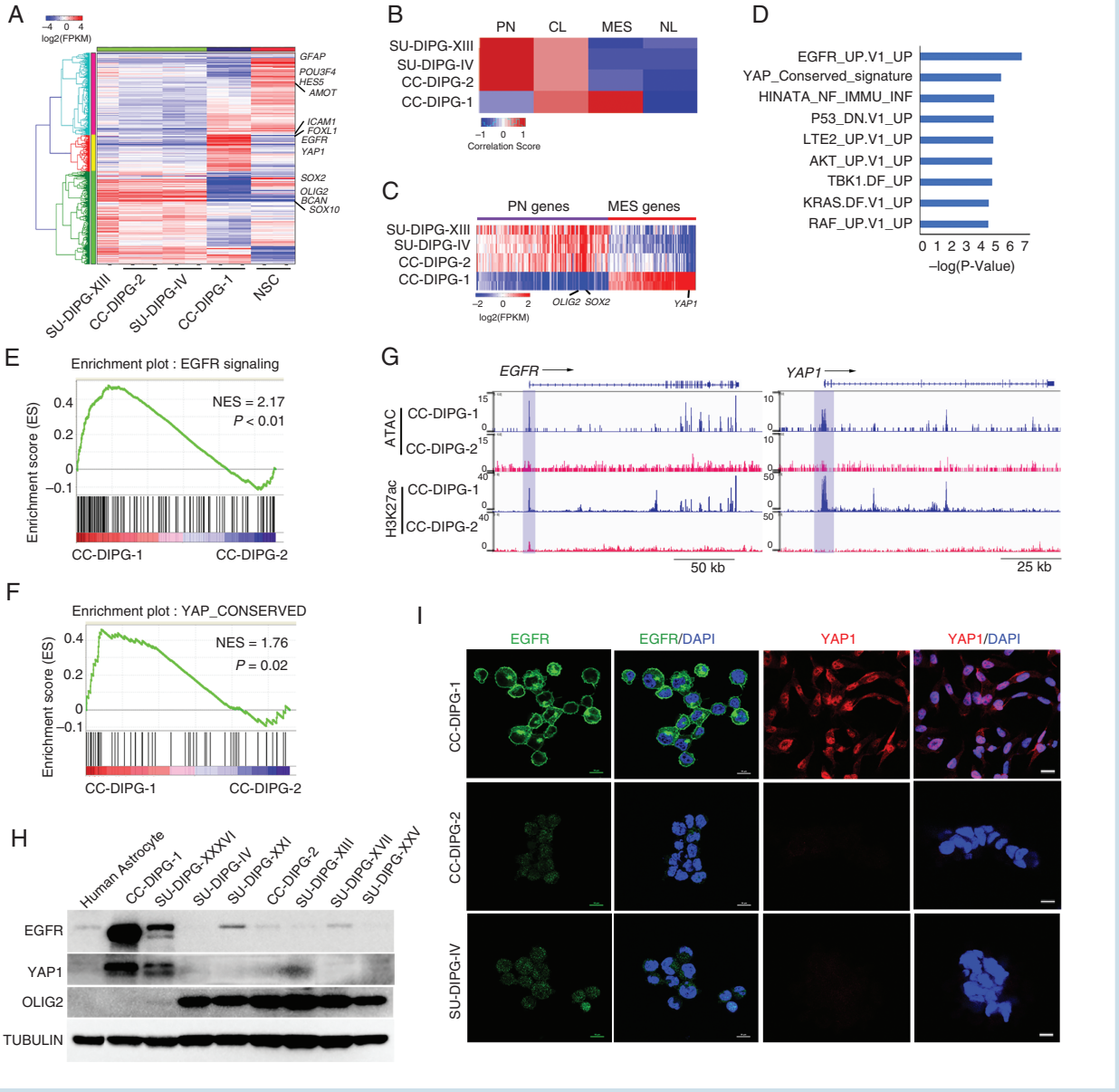

Fig. 4 CC-DIPG-1 cells have high levels of *EGFR* and *YAP1* expression. (A) Heatmap of the gene expression in DIPG cell lines and human neural stem cells (NSC). (B) Spearman correlation coefficients of gene expression patterns of DIPG cell lines with those of different GBM subtypes based on the signature genes for GBM classification in TCGA. (C) Heatmap of expression levels of the signature genes in proneural (PN) and mesenchymal (MES) GBMs that are substantially differentiated in two groups of DIPG cells. (D) Bar diagram showing signaling pathways enriched in CC-DIPG-1 cells compared with DIPG-2. (E, F) GSEA plots of (E) EGFR signaling and (F) YAP signaling signatures in CC-DIPG-1 and CC-DIPG-2 cells. (G) Chromatin accessibility and H3K27ac ChIP-seq profiles at *EGFR* and *YAP1* loci in CC-DIPG-1 and CC-DIPG-2 cells. (H) Western blot showing EGFR and YAP1 expression in indicated DIPG cells. (I) Confocal immunofluorescence microscopy images showing expression of EGFR (green) and YAP1 (red) in CC-DIPG-1, CC-DIPG-2, and SU-DIPG-IV cells. Scale bars, 10 μm. Abbreviations: DIPG, diffuse intrinsic pontine glioma; EGFR, epidermal growth factor receptor; GBM, glioblastoma.

At the chromatin level, ATAC signals were enriched at transcription start sites and in gene bodies of *YAP1* and *EGFR* loci in CC-DIPG-1 cells compared with DIPG-2 cells, and these open chromatin regions were associated with H3K27ac (Figure 4G), an activating histone mark for gene transcription.[32] In contrast to OLIG2-expressing CC-DIPG-2, SU-DIPG-IV, SU-DIPG-XXI, SU-DIPG-XIII, SU-DIPG-XVII, or SU-DIPG-XXV cells, the high expression levels of EGFR and YAP1 in OLIG2-nominal CC-DIPG-1 cells and SU-DIPG-XXXVI were confirmed by western blot (Figure 4H) and immunofluorescent staining (Figure 4I). Together, the low expression of OLIG2 and SOX2 with elevated YAP1 and EGFR expression is consistent with the mesenchymal-like phenotype of CC-DIPG-1 cells.

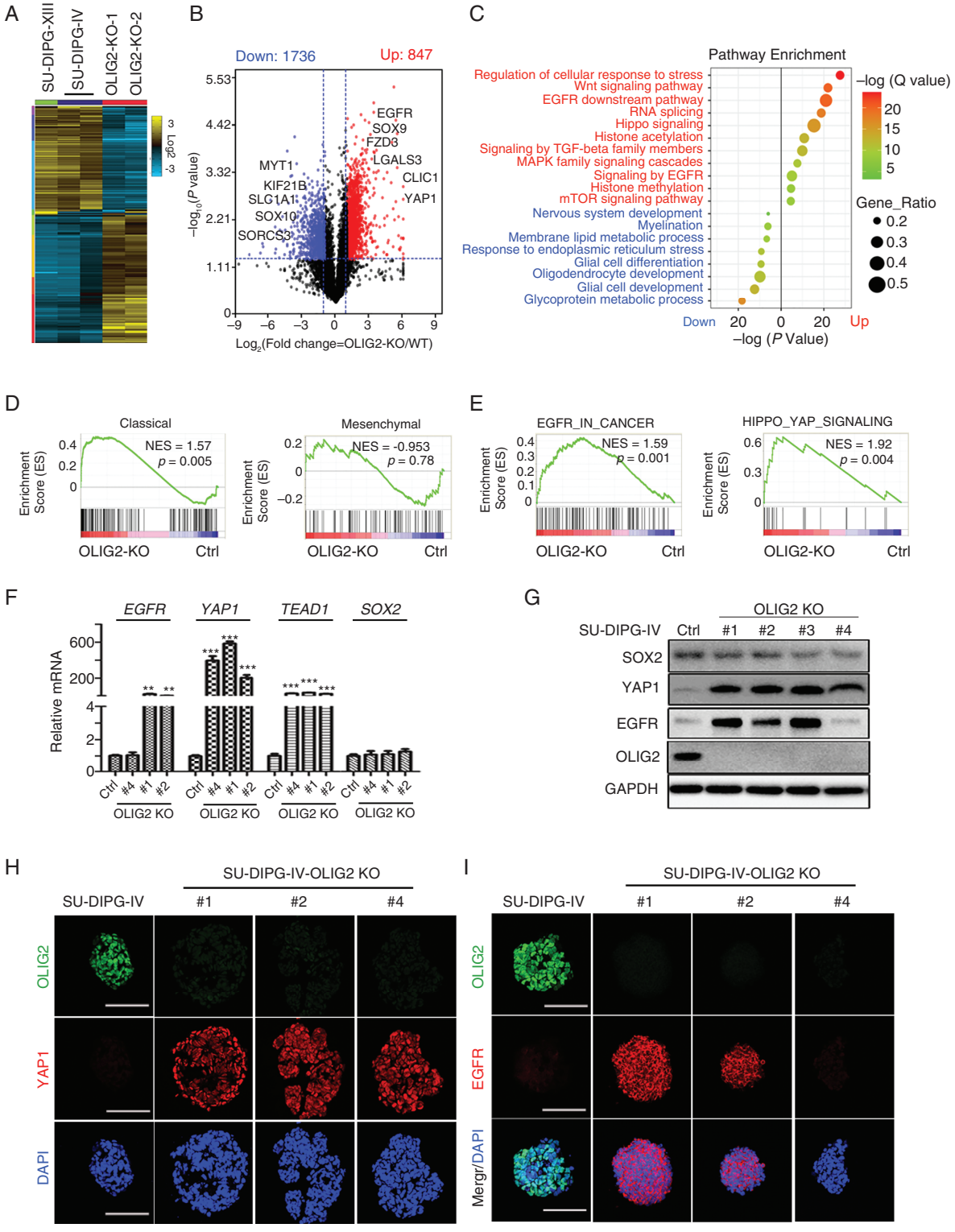

Fig. 5 Deletion of *OLIG2* causes a DIPG cell phenotype shift. (A) Heatmap of the genes differentially expressed in wild-type and *OLIG2*-KO SU-DIPG-IV and SU-DIPG-XIII cells. (B) Volcano plot of transcriptome profiles of wild-type and *OLIG2*-KO DIPG cells. Red and blue dots represent genes significantly upregulated or downregulated, respectively, in *OLIG2*-KO DIPGs compared to wild-type cells (fold change >2, $P <$ .05). (C) KEGG analysis of the upregulated and downregulated genes in *OLIG2*-KO compared with wild-type SU-DIPG-IV and SU-DIPG-XIII cells. (D, E) GSEA enrichment plots showing the comparison of gene expression profiles in wild-type proneural-like DIPG cells and *OLIG2*-KO. NES,

Deletion of *OLIG2* in Proneural-Like DIPG Cells Leads to Activation of YAP1 and EGFR Signaling and a Tumor Phenotype Shift

Previous studies showed that deletion of *OLIG2* induced a shift in tumor phenotype in a proneural GBM mouse model.[21] To determine whether OLIG2 regulates tumor phenotypes in OLIG2-expressing DIPG cell lines, we knocked out *OLIG2* in SU-DIPG-IV using the CRISPR-Cas9 system (Supplementary Figure 2). Transcriptome profiling analysis by RNA-seq identified a set of differentially expressed genes that are significantly upregulated and downregulated by more than 2-fold in *OLIG2*-KO cells compared to control wild-type cells (Figure 5A). By interrogating gene expression signatures from the Molecular Signatures Database,[33] we found that the HIPPO-YAP pathway (eg, YAP1, TEAD1/2, and FZD3), EGFR signaling, and TGF-β signaling were substantially enriched (Figure 5B and C), whereas the pathway genes associated with oligodendrocyte lineage development (eg, SOX10 and MYT1) as well as normal glial and neuronal development (eg, SLC1A1 and SORCS3) were downregulated in *OLIG2*-KO cells (Figure 5C).

GSEA of differentially regulated genes revealed a strong enrichment of classical-like GBM signature genes, but not mesenchymal signature genes, in *OLIG2*-KO cells compared with OLIG2 wild-type SU-DIPG-IV proneural-like tumor cells (Figure 5D). This is consistent with the previous observation that OLIG2 deletion resulted in a tumor phenotype transition from proneural to classical GBM in a mouse glioma model.[21] Furthermore, we found that there was a marked upregulation of HIPPO_YAP conserved signatures in addition to EGFR pathways in *OLIG2*-KO DIPG cells (Figure 5E). These observations suggest that deletion of *OLIG2* alters gene expression patterns and results in a change in the DIPG tumor cell phenotype.

qRT-PCR analyses further confirmed the upregulation of YAP1 and EGFR pathway genes in *OLIG2*-KO DIPG-IV cells (Figure 5F). In addition, when individual clones derived from single cells were examined by western blot, we found that YAP1 pathway proteins were upregulated in all subclones (4/4), and that EGFR was upregulated in a majority of individual clones (3/4) (Figure 5G). Immunostaining further confirmed the upregulation of YAP1 and EGFR in the *OLIG2*-KO DIPG-IV tumor cells (Figure 5H and I). Intriguingly, the expression of SOX2 was not significantly altered in these cells (Figure 5F and G). These data indicate that YAP1 and EGFR expression is negatively regulated by OLIG2 in proneural-like DIPG cells but that OLIG2 does not regulate SOX2 expression.

YAP1 Signaling Is Negatively Correlated With OLIG2 and Is Regulated by SOX2 in DIPG Cells

We next analyzed gene expression data of DIPG tumor tissues available in the TCGA database (GSE26576). In patients, levels of *OLIG2* and *YAP1* are negatively correlated, despite the levels of *OLIG2* and EGFR are not statistically correlated (Figure 6A and B), suggesting that *YAP1* levels are reciprocal to *OLIG2* in the DIPG tumor tissues. A recent study indicated that OLIG2 overexpression in a glioma stem cell line[34] reduced the levels of the activating histone mark H3K27ac on the promoter and enhancer elements of the *YAP1* gene locus compared with control (Figure 6C). To determine the relationship between OLIG2 and YAP1 expression in DIPG cells, we over-expressed OLIG2 using a lentiviral vector in CC-DIPG-1 cells, which expressed a high level of YAP1, and found that OLIG2 overexpression inhibited YAP1 expression, but had no apparent effect on EGFR expression (Figure 6D), suggesting that OLIG2 overexpression represses the YAP1 expression level in the DIPG cells.

SOX2 overexpression increased the signals of the H3K27ac histone mark on the promotor element of *YAP1* in the GBM cells[34] (Figure 6C). Therefore, we then examined whether SOX2 is required for YAP1 expression. shRNA-mediated *SOX2* knockdown resulted in a downregulation of *YAP1* expression in *OLIG2*-KO SU-DIPG-IV cells (Figure 6E). In addition, western blot analysis showed that *SOX2* knockdown led to a reduction of YAP1 expression in the *OLIG2*-KO SU-DIPG-IV cells (Figure 6F). To determine the role of OLIG2 and SOX2 in the DIPG cell growth, we depleted SOX2 in DIPG-IV cells using shRNA with or without *OLIG2* KO. Knockdown of *SOX2* alone did not affect cell growth compared to control cells; however, *SOX2* knockdown together with *OLIG2* KO resulted in a significant reduction of tumor cell growth (Figure 6G). These observations suggest that SOX2 and OLIG2 together are required for pro-neural-like DIPG cell proliferation.

Inhibition of YAP1 and EGFR Signaling Impairs Growth of OLIG2-Deficient DIPG Cells

Given the upregulation of EGFR and YAP1 pathways in *OLIG2*-negligible or deficient DIPG cells, we next examined whether inhibition of these pathways could impede these tumor cell proliferation. Treatment of CC-DIPG-1 cells with the EGFR inhibitor gefitinib[21] or the YAP1 inhibitor verteporfin[35] alone reduced cell growth to a certain extent (Figure 6H), while the combination of verteporfin and gefitinib substantially attenuated cell growth of CC-DIPG-1 cells (Figure 6H). Treatment with gefitinib, verteporfin,

normalized enrichment score; *P* value, represents the statistical significance of the enrichment score. (F) qRT-PCR analysis for the indicated genes in wild-type SU-DIPG-IV cells and three *OLIG2*-KO subclones. Data are presented as means ± SEM; n = 3 independent experiments; $^{*}P < .05$, $^{**}P < .01$, $^{***}P < .001$; one-way ANOVA with multiple comparisons test. (G) Representative western blots show expression of SOX2, EGFR, YAP1, and OLIG2 in wild-type and *OLIG2*-KO SU-DIPG-IV cells. GAPDH was detected as a loading control. (H-I) Confocal immunofluorescence microscopy images showing expression of (H) OLIG2 and YAP1 and (I) EGFR in wild-type DIPG-IV and *OLIG2*-KO subclones. Scale bars in H and I, 100 μm. Abbreviations: DIPG, diffuse intrinsic pontine glioma; GSEA, gene set enrichment analysis; OLIG2, oligodendrocyte transcription factor 2; qRT-PCR, quantitative RT-PCR.

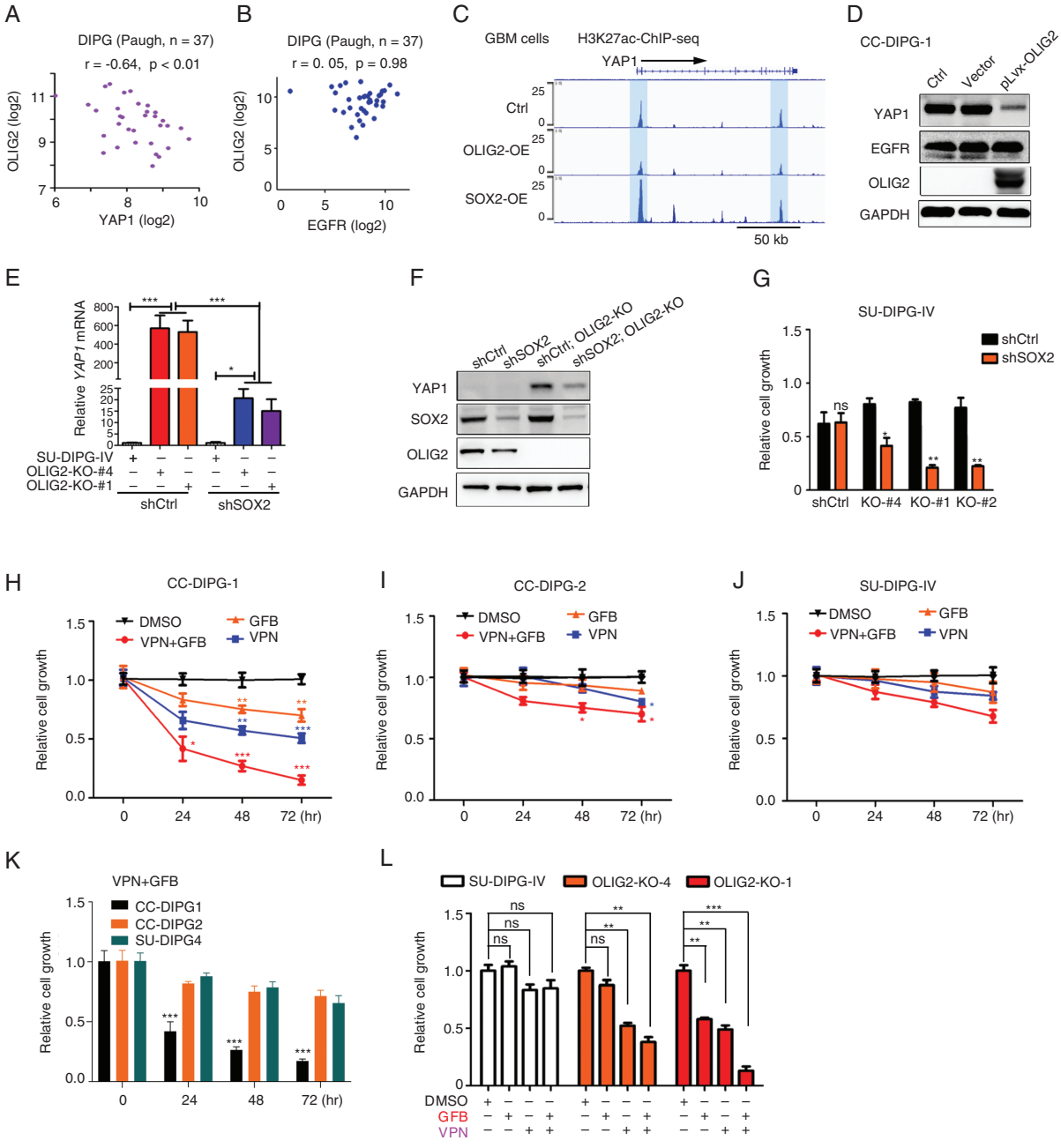

Fig. 6 Targeting OLIG2/SOX2 and YAP1/EGFR signaling inhibits the growth of DIPG cells. (A, B) The correlations of *OLIG2* expression with (A) *YAP1* and (B) *EGFR* expression in DIPG tumor tissues. *r*, correlation score; *P* value, statistical significance of the correlation score. (C) H3K27ac signal over the *YAP1* locus in control, OLIG2-overexpressing, or SOX2-overexpressing differentiated GBM cells. (D) Representative western blots for EGFR, YAP1, and OLIG2 in control and CC-DIPG-1 cells that over-express OLIG2. GAPDH was detected as a loading control. (E) qRT-PCR analysis of *YAP1* in wild-type SU-DIPG-IV cells and *OLIG2*-KO subclones with and without shSOX2 expression. Data are presented as means ± SEM; n = 3 independent experiments; $^{*}P < .05$, $^{**}P < .01$; $^{***}P < .001$; one-way ANOVA with multiple comparisons test. (F) Representative western blots show for SOX2, YAP1, and OLIG2 in wild-type SU-DIPG-IV and *OLIG2*-KO subclones with and without shSOX2 expression. GAPDH was detected as a loading control. (G) Proliferation of wild-type DIPG-IV cells and *OLIG2*-KO subclones with and without shSOX2 expression determined using the WST-1 assay. Data are presented as means ± SEM; n = 3 independent experiments; $^{*}P < .05$, $^{**}P < .01$; $^{***}P < .001$; two-tailed Student's *t*-test. (H) Cell growth of CC-DIPG-1, CC-DIPG-2, and SU-DIPG-IV cells treated with gefitinib (GFB) or verteporfin (VPN) or the combination (VPN + GFB) at the indicated times after treatment initiation. Data are presented as means ± SEM; n = 3 independent experiments; $^{*}P < .05$, $^{**}P < .01$, $^{***}P < .001$; one-way ANOVA with multiple comparisons test. (I) Cell growth of CC-DIPG-1, CC-DIPG-2, and SU-DIPG-IV cells after treatment with the combination of gefitinib and verteporfin. Data are presented as means ± SEM; n = 3 independent experiments; $^{*}P < .05$, one-way ANOVA with multiple comparisons test. (J) Cell growth of DIPG-IV and its *OLIG2*-KO subclones treated with gefitinib and verteporfin or the combination for 72 h. Data are presented as means ± SEM; n = 3 independent experiments; $^{**}P < .01$, $^{***}P < .001$; one-way ANOVA with multiple comparisons test. Abbreviations: DIPG, diffuse intrinsic pontine glioma; EGFR, epidermal growth factor receptor; qRT-PCR, quantitative RT-PCR.

and the combination did not substantially inhibit the expansion of OLIG2-expressing CC-DIPG-2 and SU-DIPG-IV cells with low EGFR and YAP1 signaling (Figure 6I and J). Moreover, the combined treatment with verteporfin and gefitinib more strongly inhibited cell proliferation of OLIG2-nominal CC-DIPG-1 cells than OLIG2-expressing CC-DIPG-2 and SU-DIPG-IV cells (Figure 6K). Further, the proliferation of *OLIG2*-KO SU-DIPG-IV cells was more strongly attenuated by combined verteporfin and gefitinib treatment than was the growth of the wild-type SU-DIPG-IV cells (Figure 6L). These results suggest that OLIG2 nominal or deficient DIPG cells are more sensitive to inhibition of adaptive EGFR and YAP1 signaling.

Discussion

Our studies reveal that DIPG cells are highly heterogeneous and exhibit distinct tumor phenotypes. Although most DIPG cell lines resemble the proneural subtype of high-grade gliomas, a set of DIPG cell lines, such as CC-DIPG-1, SU-DIPG-XXXIII, and DIPG-XXXVI, lack or have low levels of OLIG2 expression and exhibit mesenchymal-like or classical-like phenotypes, suggesting that different DIPG tumor cells with unique molecular signatures might be derived from distinct lineage cells of origin. Our observations of negligible OLIG2 expression in CC-DIPG-1 cells do not agree with a previous report[24] that OLIG2 is important for CC-DIPG-1 cell growth. In addition, CRISPR-Cas9 KO of *OLIG2* in OLIG2-expressing SU-DIPG-IV and CC-DIPG-2 cells did not substantially impair tumor cell proliferation. Thus, our data indicate that OLIG2 is not essentially required for maintaining tumor cell growth in the DIPG cell lines tested. In the previous report, the lentivirally expressed shRNA was designed to inhibit OLIG2 expression in the OLIG2-nominal CC-DIPG-1 cells,[24] however, OLIG2 knockdown was not shown for CCHMC-DIPG-1 cells. We hypothesize that the shRNA used in the Anderson et al.'s study had off-target effects.

Although the patient tumor tissues, from which CC-DIPG-1 was initially isolated, showed OLIG2 immunoreactivity in some cell populations (data not shown), the CC-DIPG-1 cell line derived from this tissue exhibited minimal OLIG2 expression. DIPG tumors are heterogeneous, and distinct tumorigenic subpopulations have been detected in DIPG tumors isolated from patients.[17,28] Thus, the minimal OLIG2 expression in CC-DIPG-1 cells might be due in part to subclonal selection during the culture or from different tumor cell populations within the tumor tissues.

The precise mechanism of *OLIG2* silencing in CC-DIPG-1 cells is not known. Our whole-genome DNA methylation profiling revealed that the promoter and gene body elements of *OLIG2* are hypermethylated in CC-DIPG-1 cells. Indeed, DNA demethylation by decitabine treatment results in re-expression and upregulation of OLIG2 in CC-DIPG-1 cells, suggesting that DNA hypermethylation contributes to OLIG2 silencing. However, decitabine treatment did not alter the expression of YAP1 and EGFR substantially (Supplementary Figure 1B). This might be in part due to the moderate increase of OLIG2 levels after decitabine treatment compared with the expression level of OLIG2 in other OLIG2-expressing DIPG cells (Supplementary Figure 1A), which may not be sufficient to repress the expression of *YAP1* and *EGFR*. The exact mechanisms underlying YAP1 and EGFR expression remain to be determined. In addition, the chromatin landscape assessed by ATAC-seq indicates that the *OLIG2* locus is not accessible in CC-DIPG-1 cells. Thus, these two features of epigenetic silencing by DNA hypermethylation and chromatin inaccessibility likely contribute to the negligible OLIG2 expression observed in CC-DIPG-1 cells. OLIG2 expression was absent or minimal in early and late passage cells, suggesting that the loss of OLIG2 expression is intrinsic to CC-DIPG-1 cells.

In contrast to the DNA methylation pattern in the *OLIG2* locus in CC-DIPG-1 cells, the methylation level of the *EGFR* locus was comparable to the DIPG cell lines evaluated (data not shown), indicating that elevation of EGFR levels in CC-DIPG-1 cells is independent of DNA methylation regulation. At present, it is not clear whether or how H3.3K27M or H3.1K27M mutations influence OLIG2 expression in DIPG cells.

It is worth noting that OLIG2-nominal CC-DIPG-1 cells proliferate more rapidly than other DIPG cell lines tested (Figure 3A). Elevation of both EGFR and YAP1 signaling, which are often associated with more aggressive and therapy-resistant human cancers,[36] likely contribute to this rapid growth phenotype. Notably, based on the gene expression profiles, *OLIG2* deletion in proneural-like DIPG cells led to the upregulation of YAP1 and EGFR signaling, suggesting a phenotypic transition from proneural to a mesenchymal-like or classical-like tumor signature in the absence of OLIG2. A similar tumor phenotype shift caused by OLIG2 loss in murine GBM cells[21] suggests a conserved role of OLIG2 in regulating tumor phenotypes in both GBM and DIPG cells.

Transcriptomic analysis revealed an activation of HIPPO-YAP and EGFR pathways in OLIG2-deficient tumors. Targeting of EGFR and YAP1 signaling with pharmacological inhibitors suppressed the growth of OLIG2-deficient DIPG cell lines and *OLIG2*-KO DIPG cells. This indicates that OLIG2 inhibition can lead to the sensitization of DIPG cells to inhibitors of EGFR and YAP1 signaling, which confer a therapeutic vulnerability in these DIPG cells. Combined inhibition of HIPPO-YAP1 and EGFR signaling might offer an approach for targeting and inhibiting the growth of OLIG2-nominal or deficient DIPG cells, though in vivo therapeutic efficacy of EGFR/YAP inhibition on OLIG2-WT and OLIG2-deficient DIPG cells remains to be determined. This observation might also have an implication for targeting therapy-resistant aggressive mesenchymal human malignant gliomas, which express low levels of OLIG2.[37]

In summary, in contrast to the previous report, our data shown here indicate that OLIG2 is hardly detectable in the mesenchymal-like CC-DIPG-1 cells. KO of *OLIG2* in OLIG2-expressing DIPG cells suggests that OLIG2 is not essentially required for maintaining proliferation in the tested DIPG cell lines, while OLIG2 deficiency or deletion leads to a shift of the tumor phenotype identity in the DIPG cells with elevation of EGFR and YAP1 signaling. However, our results do not address whether OLIG2 is required for the initiation of DIPG tumorigenesis. It is possible that OLIG2 has

a stage-dependent function during DIPG tumor development and progression. Although it has been shown the OLIG2 is important for glioma initiation during tumorigenesis in a murine model of GBM,[21] much work remains to be done in order to understand the function of OLIG2 in DIPG tumorigenesis, progression, and maintenance.

Supplementary Material

Supplementary material is available at *Neuro-Oncology* online.

Keywords

diffuse intrinsic pontine glioma (DIPG) | distinct DIPG tumor phenotypes | genomic landscapes | OLIG2 | YAP1 and EGFR signaling

Funding

This research was supported by the CancerFree KIDS Foundation.

Acknowledgments

The authors would like to thank Dr. Michelle Monje at Stanford University for providing the DIPG cell lines and Sean Ogurek for technical support.

Conflict of interest statement. The authors declare no conflict of interest.

Authorship statement. Conception and design: Y.L., Z.L., Y.D., R.D., and Q.R.L. Data acquisition, analysis, and interpretation: Y.L., Z.L., Y.D., F.Z., R.R., J.W., L.X., S.S.K., S.S., M.D.S., K.B., M.G., M.F., and R.D. Writing and review: Y.L., Z.L., Y.D., R.R., R.D., and Q.R.L. Study supervision: Q.R.L.

Data and software availability

All the high-throughput data have been deposited in the NCBI Gene Expression Omnibus (GEO) under accession number GEO: GSE157158.

References

1. Donaldson SS, Laningham F, Fisher PG. Advances toward an understanding of brainstem gliomas. *J Clin Oncol*. 2006;24(8):1266–1272.
2. Hargrave D, Bartels U, Bouffet E. Diffuse brainstem glioma in children: critical review of clinical trials. *Lancet Oncol*. 2006;7(3):241–248.
3. Tate MC, Lindquist RA, Nguyen T, et al. Postnatal growth of the human pons: a morphometric and immunohistochemical analysis. *J Comp Neurol*. 2015;523(3):449–462.
4. Johung TB, Monje M. Diffuse intrinsic pontine glioma: new pathophysiological insights and emerging therapeutic targets. *Curr Neuropharmacol*. 2017;15(1):88–97.
5. Monje M, Mitra SS, Freret ME, et al. Hedgehog-responsive candidate cell of origin for diffuse intrinsic pontine glioma. *Proc Natl Acad Sci U S A*. 2011;108(11):4453–4458.
6. Ballester LY, Wang Z, Shandilya S, et al. Morphologic characteristics and immunohistochemical profile of diffuse intrinsic pontine gliomas. *Am J Surg Pathol*. 2013;37(9):1357–1364.
7. Mackay A, Burford A, Carvalho D, et al. Integrated molecular meta-analysis of 1,000 pediatric high-grade and diffuse intrinsic pontine glioma. *Cancer Cell*. 2017;32(4):520–537.e5.
8. Puget S, Philippe C, Bax DA, et al. Mesenchymal transition and PDGFRA amplification/mutation are key distinct oncogenic events in pediatric diffuse intrinsic pontine gliomas. *PLoS One*. 2012;7(2):e30313.
9. Zarghooni M, Bartels U, Lee E, et al. Whole-genome profiling of pediatric diffuse intrinsic pontine gliomas highlights platelet-derived growth factor receptor alpha and poly (ADP-ribose) polymerase as potential therapeutic targets. *J Clin Oncol*. 2010;28(8):1337–1344.
10. Larson JD, Kasper LH, Paugh BS, et al. Histone H3.3 K27M accelerates spontaneous brainstem glioma and drives restricted changes in bivalent gene expression. *Cancer Cell*. 2019;35(1):140–155.e7.
11. Pathania M, De Jay N, Maestro N, et al. H3.3(K27M) cooperates with Trp53 loss and PDGFRA gain in mouse embryonic neural progenitor cells to induce invasive high-grade gliomas. *Cancer Cell*. 2017;32(5):684–700.e9.
12. Verhaak RG, Hoadley KA, Purdom E, et al.; Cancer Genome Atlas Research Network. Integrated genomic analysis identifies clinically relevant subtypes of glioblastoma characterized by abnormalities in PDGFRA, IDH1, EGFR, and NF1. *Cancer Cell*. 2010;17(1):98–110.
13. MacDonald TJ, Aguilera D, Kramm CM. Treatment of high-grade glioma in children and adolescents. *Neuro Oncol*. 2011;13(10):1049–1058.
14. Patel AP, Tirosh I, Trombetta JJ, et al. Single-cell RNA-seq highlights intratumoral heterogeneity in primary glioblastoma. *Science*. 2014;344(6190):1396–1401.
15. Tirosh I, Venteicher AS, Hebert C, et al. Single-cell RNA-seq supports a developmental hierarchy in human oligodendroglioma. *Nature*. 2016;539(7628):309–313.
16. Venteicher AS, Tirosh I, Hebert C, et al. Decoupling genetics, lineages, and microenvironment in IDH-mutant gliomas by single-cell RNA-seq. *Science*. 2017;355(6332):eaai8478.
17. Filbin MG, Tirosh I, Hovestadt V, et al. Developmental and oncogenic programs in H3K27M gliomas dissected by single-cell RNA-seq. *Science*. 2018;360(6386):331–335.
18. Nagaraja S, Vitanza NA, Woo PJ, et al. Transcriptional dependencies in diffuse intrinsic pontine glioma. *Cancer Cell*. 2017;31(5):635–652.e6.

19. Lu QR, Sun T, Zhu Z, et al. Common developmental requirement for Olig function indicates a motor neuron/oligodendrocyte connection. *Cell*. 2002;109(1):75–86.
20. Zhou Q, Anderson DJ. The bHLH transcription factors OLIG2 and OLIG1 couple neuronal and glial subtype specification. *Cell*. 2002;109(1):61–73.
21. Lu F, Chen Y, Zhao C, et al. Olig2-dependent reciprocal shift in PDGF and EGF receptor signaling regulates tumor phenotype and mitotic growth in malignant glioma. *Cancer Cell*. 2016;29(5):669–683.
22. Weng Q, Wang J, Wang J, et al. Single-cell transcriptomics uncovers glial progenitor diversity and cell fate determinants during development and gliomagenesis. *Cell Stem Cell*. 2019;24(5):707–723.e8.
23. Khuong-Quang DA, Buczkowicz P, Rakopoulos P, et al. K27M mutation in histone H3.3 defines clinically and biologically distinct subgroups of pediatric diffuse intrinsic pontine gliomas. *Acta Neuropathol*. 2012;124(3):439–447.
24. Anderson JL, Muraleedharan R, Oatman N, et al. The transcription factor Olig2 is important for the biology of diffuse intrinsic pontine gliomas. *Neuro Oncol*. 2017;19(8):1068–1078.
25. Grasso CS, Tang Y, Truffaux N, et al. Functionally defined therapeutic targets in diffuse intrinsic pontine glioma. *Nat Med*. 2015;21(7):827.
26. Buenrostro JD, Wu B, Chang HY, Greenleaf WJ. ATAC-seq: a method for assaying chromatin accessibility genome-wide. *Curr Protoc Mol Biol*. 2015;109:21.29.1–21.29.9.
27. Boyle P, Clement K, Gu H, et al. Gel-free multiplexed reduced representation bisulfite sequencing for large-scale DNA methylation profiling. *Genome Biol*. 2012;13(10):R92.
28. Vinci M, Burford A, Molinari V, et al. Functional diversity and cooperativity between subclonal populations of pediatric glioblastoma and diffuse intrinsic pontine glioma cells. *Nat Med*. 2018;24(8):1204–1215.
29. Vaissière T, Sawan C, Herceg Z. Epigenetic interplay between histone modifications and DNA methylation in gene silencing. *Mutat Res*. 2008;659(1–2):40–48.
30. Yalcin A, Kovarbasic M, Wehrle J, et al. The oligodendrocyte lineage transcription factor 2 (OLIG2) is epigenetically regulated in acute myeloid leukemia. *Exp Hematol*. 2017;55:76–85.e3.
31. Sanjana NE, Shalem O, Zhang F. Improved vectors and genome-wide libraries for CRISPR screening. *Nat Methods*. 2014;11(8):783–784.
32. Bernstein BE, Mikkelsen TS, Xie X, et al. A bivalent chromatin structure marks key developmental genes in embryonic stem cells. *Cell*. 2006;125(2):315–326.
33. Subramanian A, Tamayo P, Mootha VK, et al. Gene set enrichment analysis: a knowledge-based approach for interpreting genome-wide expression profiles. *Proc Natl Acad Sci U S A*. 2005;102(43):15545–15550.
34. Suvà ML, Rheinbay E, Gillespie SM, et al. Reconstructing and reprogramming the tumor-propagating potential of glioblastoma stem-like cells. *Cell*. 2014;157(3):580–594.
35. Wu LMN, Deng Y, Wang J, et al. Programming of Schwann cells by Lats1/2-TAZ/YAP signaling drives malignant peripheral nerve sheath tumorigenesis. *Cancer Cell*. 2018;33(2):292–308.e7.
36. Thompson BJ. YAP/TAZ: drivers of tumor growth, metastasis, and resistance to therapy. *Bioessays*. 2020;42(5):e1900162.
37. Olar A, Aldape KD. Using the molecular classification of glioblastoma to inform personalized treatment. *J Pathol*. 2014;232(2):165–177.